
This is an electronic reprint of the original article.
This reprint may differ from the original in pagination and typographic detail.

Nguyen, Minh Truong Xuan; Nguyen, Kha; Pham, Phuong Thi Thuy; Huynh, Ha Ky Phuong ;
Nguyen, Son Truong

Pd coated one-dimensional Ag nanostructures: Controllable architecture and their electrocatalytic performance for ethanol oxidation in alkaline media

Published in:
International Journal of Hydrogen Energy

DOI:
[10.1016/j.ijhydene.2020.10.226](https://doi.org/10.1016/j.ijhydene.2020.10.226)

Published: 19/01/2021

Document Version
Peer-reviewed accepted author manuscript, also known as Final accepted manuscript or Post-print

Please cite the original version:
Nguyen, M. T. X., Nguyen, K., Pham, P. T. T., Huynh, H. K. P., & Nguyen, S. T. (2021). Pd coated one-dimensional Ag nanostructures: Controllable architecture and their electrocatalytic performance for ethanol oxidation in alkaline media. *International Journal of Hydrogen Energy*, 46(5), 3909-3921.
<https://doi.org/10.1016/j.ijhydene.2020.10.226>

This material is protected by copyright and other intellectual property rights, and duplication or sale of all or part of any of the repository collections is not permitted, except that material may be duplicated by you for your research use or educational purposes in electronic or print form. You must obtain permission for any other use. Electronic or print copies may not be offered, whether for sale or otherwise to anyone who is not an authorised user.

International Journal of Hydrogen Energy

Pd coated one-dimensional Ag nanostructures: Controllable architecture and their electrocatalytic performance for ethanol oxidation in alkaline media

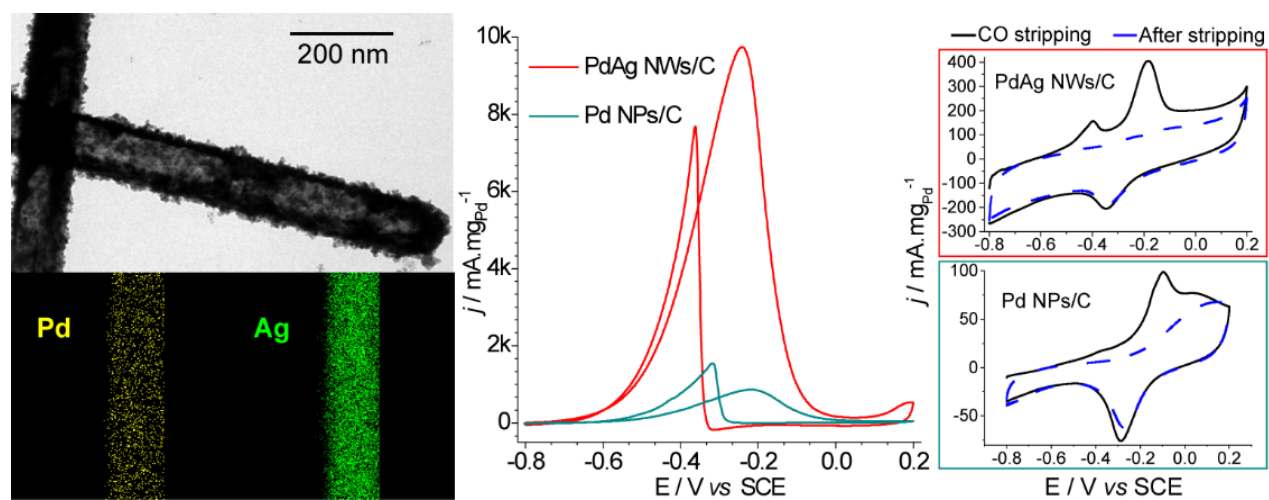
--Accepted Manuscript--

Manuscript Number:	HE-D-20-02731R5
Article Type:	Full Length Article
Section/Category:	Catalysts / Electrocatalysts / Photocatalysts
Keywords:	PdAg nanowires; low Pd-loading; core-shell; direct ethanol fuel cells; electrochemical durability; CO poisoning tolerance.
Corresponding Author:	Son Truong Nguyen, Ph.D. Ho Chi Minh City University of Technology Ho Chi Minh City, VIET NAM
First Author:	Minh T Nguyen
Order of Authors:	Minh T Nguyen Kha M Nguyen, PhD Phuong T Pham, PhD Ha K Huynh, PhD Son Truong Nguyen, Ph.D.
Abstract:	<p>One-dimensional (1D) metal-coated Pd structures are efficient catalysts for the ethanol electro-oxidation and promising strategy for minimizing the Pd-loading toward commercialization of direct ethanol fuel cells (DEFCs). Herein, the decorated and core-shell architectures of a novel Pd coating on Ag nanowires (PdAg-NWs) are controllable by a two-step polyol method based on the galvanic replacement reaction. The integration of uniform shell with a low Pd concentration and partial hollow structure onto 1D PdAg-NWs exhibits the highest efficiency for ethanol oxidation reaction (EOR) in alkaline solution. In comparison with Pd nanoparticles (PdNPs/C), the PdAgNWs/C performs 11 times superior EOR activity, and the onset potential shifts 80 mV negatively. The presence of Ag in PdAg-NWs enhances the absorption capacity of ethanol molecules and hydroxyl ions on the active sites, and improves the catalyst tolerance to CO-like intermediates, making them a potential anodic catalyst for DEFCs.</p>

Graphical abstract:

Pd coated one-dimensional Ag nanostructures: Controllable architecture and their electrocatalytic performance for ethanol oxidation in alkaline media

Minh Truong Xuan Nguyen, Minh-Kha Nguyen, Phuong Thi Thuy Pham, Ha Ky Phuong Huynh, Son Truong Nguyen



Highlights:

- Novel PdAg core-shell nanowires with a low Pd-loading were synthesized.
- Controllable configuration of Pd layer by temperature and PVP concentration.
- Adjustable particle size of Pd by reaction time and Pd/Ag molar ratio.
- Efficient bifunctional electrocatalyst for direct ethanol fuel cells in alkaline media.

**Pd coated one-dimensional Ag nanostructures: Controllable architecture
and their electrocatalytic performance for ethanol oxidation in alkaline
media**

Minh Truong Xuan Nguyen^{1,3}, Minh-Kha Nguyen^{1,3,4}, Phuong Thi Thuy Pham⁵, Ha Ky

Phuong Huynh^{1,3}, Son Truong Nguyen^{1,2,3,*}

¹*Faculty of Chemical Engineering, Ho Chi Minh City University of Technology (HCMUT), 268 Ly Thuong Kiet St., Dist. 10, Ho Chi Minh City, Vietnam*

²*Research Institute for Sustainable Energy, Ho Chi Minh City University of Technology (HCMUT), 268 Ly Thuong Kiet St., Dist. 10, Ho Chi Minh City, Vietnam*

³*Vietnam National University Ho Chi Minh City, Linh Trung Ward, Thu Duc Dist., Ho Chi Minh City, Vietnam*

⁴*Department of Neuroscience and Biomedical Engineering, Aalto University School of Science, P.O. Box 12200, FI-00076 Aalto, Finland*

⁵*Institute of Chemical Technology - Vietnam Academy of Science and Technology, TL29 St., Thanh Loc Ward, Dist. 12, Ho Chi Minh City, Vietnam*

* Corresponding author: ntson@hcmut.edu.vn

Abstract

One-dimensional (1D) metal-coated Pd structures are efficient catalysts for the ethanol electro-oxidation and promising strategy for minimizing the Pd-loading toward commercialization of direct ethanol fuel cells (DEFCs). Herein, the decorated and core-shell architectures of a novel Pd coating on Ag nanowires (PdAg-NWs) are controllable by a two-step polyol method based on the galvanic replacement reaction. The integration of uniform shell with a low Pd concentration and partial hollow structure onto 1D PdAg-NWs exhibits the highest efficiency for ethanol oxidation reaction (EOR) in alkaline solution. In comparison with Pd nanoparticles (PdNPs/C), the PdAgNWs/C performs 11 times superior EOR activity, and the onset potential shifts 80 mV negatively. The presence of Ag in PdAg-NWs enhances the absorption capacity of ethanol molecules and hydroxyl ions on the active sites, and improves the catalyst tolerance to CO-like intermediates, making them a potential anodic catalyst for DEFCs.

Keywords: PdAg nanowires, low Pd-loading, core-shell, direct ethanol fuel cells, electrochemical durability, CO poisoning tolerance

1. Introduction

The overconsumption of energy based on fossil fuels has generated threats to life and health of human beings, e.g., environmental pollution, greenhouse effects, global climate change and even oil competing conflicts. Therefore, renewable energy sources have been attracting many researches and considering as a new generation energy. Direct ethanol fuel cells (DEFCs), i.e., one of the most promising technology for energy conversion, environmentally friendliness and low-emission, have brought increasing level of attention in recent years [1, 2]. The complete oxidation of ethanol to CO₂ releases 12 electrons (2 electrons for formic acid electro-oxidation and 6 electrons for methanol electro-oxidation), and ethanol is considerably less toxic and can be collected from bioethanol sources. Platinum (Pt) nanomaterials is known as the most active and common anodic catalysts for alcohol electro-oxidation reactions in acidic media [3, 4]. However, recent studies [5, 6] have shown some limitations of Pt including the incomplete oxidation of alcohol producing by-products, e.g., carbon monoxide (CO), which attach to active catalytic sites. This causes catalyst self-poisoning and prevents the oxidation process. In addition, the poor Pt sources as well as its high cost have hindered the commercialization of fuel cells [7-9]. The complete oxidation of ethanol also needs high overpotentials to break the C–C bond [10]. It is confirmed that palladium (Pd) exhibits a more efficient performance for the ethanol oxidation reaction (EOR) in alkaline solution than Pt [11-14]. The adsorption of OH⁻ ions on the catalysts' surfaces in EOR can accelerate the removal of intermediates, thereby significant improvement in electrochemical active surface area [15, 16]. Pd and Pd-based nanoparticles have been considered being one of the most significant replacements for Pt electrocatalysts towards ethanol electrooxidation in alkaline condition.

The composition, structure and morphology of the catalytic materials show a strong influence in the electrocatalytic EOR performances. The combinations of Pd with other cheaper transition metals, e.g., Pb [17], Cu [18], Sn [19], Tb [20], Ni [21] and Ag [15, 22, 23], have not only minimized an amount of Pd precursors in the catalytic synthesis but also improved a

conversion of the intermediates into stable forms in EOR. Remarkably, Ag is one of the most efficient second metal to combine with Pd due to the small lattice mismatch between Pd and Ag, its excellent electrical conductivity, more oxophilic property and easy abundant storage [15, 24]. Our previous study found that the CO tolerance and stability of PdAg/C for ethanol oxidation is better than Pt/C and Pd/C [22]. The high EOR electrocatalytic activity and a superior stability of various PdAg nanostructures have also been confirmed by many recent works [16, 24]. The benefit of additional Ag suggested in a bifunctional mechanism is its acceleration on removing CO-like intermediates from the nanostructured surfaces [22, 25, 26]. The synergistic effect of Ag surface atoms in PdAg nanostructures can modify the electronic structure of Pd, supporting upshifting the d-band center of Pd [27-29]. This behaviour can promote an amount of the adsorbed hydroxyl ions as well as ethanol molecules on PdAg catalyst in alkaline electrolyte, and hence, improve the rate of EOR and the elimination of ethoxy intermediates [24, 30]. The impressive EOR activities and the high poison tolerance of the bimetallic PdAg nanostructures would be promising strategies in designing high efficient anodic catalysts for the alkaline DEFCs.

Over the past decades, various morphologies, sizes and structures of the bimetallic PdAg catalysts have been fabricated and applied for EOR in alkaline electrolyte, e.g., single-crystalline alloyed nanospheres and nanowires [16, 31], nanodendrites [13, 27], hollow raspberry-like and porous flower-shaped nanospheres [6, 32], core-shell worm-like networks [24, 33], and nanotubes [34, 35]. These studies indicate that small spherical nanomaterials with large surface energy makes them easily soluble and agglomerate into large particles during the fuel cell operation process [23, 36-39]. In comparison with zero-dimensional (0D) particles, one-dimensional (1D) nanostructured materials, e.g., nanorods and nanowires (NWs), represent a morphology paradigm associated with their fewer lattice boundaries as well as facilitating the electron transport. Despite these advantages, less attention has been given to control the configuration, i.e., decorated or core-shell, of Pd coating on 1D Ag nanostructures and evaluate

their EOR activities. Moreover, in order to synthesize PdAg nanostructures as a catalyst for EOR, current researches have operated at high Pd/Ag molar ratios from 1:3 to 1:1 [15, 16, 32, 40-42]. Meanwhile, it is informed that the Pt or Pd particles, which are inner the catalyst, show no contribution in the catalytic activities [43, 44]. These drawbacks provided us a motivation for synthesis novelty nanowire materials, in which the interior Pd part would be replaced by a cheap metal core for minimizing the Pd utilization as well as promoting the electro-catalytic abilities.

In this study, the Pd coated Ag nanowires (PdAg-NWs) catalysts were prepared at low Pd-loadings, i.e., the Pd/Ag molar ratios from 6:100 to 14:100, by the galvanic replacement reaction in ethylene glycol (EG), which offered several advantages. First and foremost, the degrees of Pd coating on AgNWs from the decorated to core-shell structures were facilely controlled by conducting the synthesis conditions, e.g., synthesis temperature, reaction duration, Pd/Ag ratios and PVP concentration. Second, the reduction of Pd²⁺ ions and deposition of Pd atoms occurred directly on the AgNWs' surface, which eliminated the formation of free Pd nanoparticles (PdNPs) in solution. Third, preparation and reaction of precursors in EG, i.e., a non-aqueous solution, can prevent the hydrolysis of Pd²⁺ ions. Fourth, AgNW-core with high electrical conductivity generates 1D electrode nanostructure and enhances the mass transport of C₂H₅OH and OH⁻, resulting in a higher electro-catalyst activity. The highly efficient bifunctional PdAg-NWs catalyst was clarified based on the electrocatalytic performances towards EOR in alkaline DEFCs as well as via CO tolerance.

2. Experimental

2.1. Materials

Potassium bromide (KBr, 99%), sodium chloride (NaCl, 99.5%), palladium(II) nitrate dihydrate (Pd(NO₃)₂·2H₂O, 99%), ethylene glycol (EG, 99.5%), polyvinylpyrrolidone (PVP, Mw ≈ 40000), silver nitrate (AgNO₃, 99%), ethanol (99.5%), alumina powder (Al₂O₃) and

Nafion solution in a mixture of water and isopropanol (5 wt.%) were obtained from Sigma Aldrich (Singapore). Carbon black (XC72) was purchased from Cabot Corp. (USA).

2.2. *Synthesis of Ag nanowires*

Ag nanowires (AgNWs) were prepared by a polyol method with EG as a solvent and a reducing agent. Typically, 0.6251 g PVP and 10 mL of EG were dissolved in a round bottom flask and heated to 150 °C under magnetic stirring. After the temperature reached constant, 100 μ L of KBr in EG (0.1 mM) was added into the mixture. After stirring for 3 min, 100 μ L of NaCl in EG (0.1 mM) was injected. Next, 3 mL of AgNO₃ in EG (0.4 M) was injected dropwise into the solution with continuous stirring for 6 min. After 120 min at 150 °C, the growth was quenched by cooling the reaction flask to room temperature. The AgNWs were purified by washing with ethanol and a centrifugation at 3000 rpm for 20 min. The purification step was repeated several times.

2.3. *Synthesis of Pd coated AgNWs*

Pd coated AgNWs (PdAg-NWs), i.e., decorated and core-shell structures, were synthesized at different reaction temperatures from 60 to 100 °C for various reaction times from 60 to 180 min as described below. The details of each investigated parameter were reported in the Supporting Information. For the sample preparation at 90 °C for 120 min, AgNWs and 10 mL of EG were mixed and heated under stirring until the mixture achieved 90 °C. 2 mL of Pd(NO₃)₂ aqueous solution (with a 1:10 molar ratio of Pd/Ag, based on initial amount of metal salts) and PVP (0.3% w/v per 12 mL of the experimental mixture) were added dropwise into the reaction flask for 20 min. Then the solution was stirred for 120 min at 90 °C. The sample was centrifuged and dried at 60 °C overnight in a vacuum oven.

2.4. *Synthesis of Pd nanoparticles*

The protocol for 3.5 nm PdNPs ([Fig. S1](#)) synthesis is adapted from previously established protocol [\[45\]](#) with minor modifications. Typically, 5 mL of EG was heated to 120 °C. Next, 3

mL of Pd(NO₃)₂ aqueous solution (30 mM) and 3 mL of PVP in EG (15.3 mg/mL) were added, simultaneously, and the reaction solution was continually stirred at 120 °C. After 60 min, the sample was collected by centrifugation and dried at 60 °C overnight in a vacuum oven.

2.5. Catalyst preparation

PdAg-NWs or PdNPs were mixed with XC72 at a 1:4 mass ratio and ethanol by stirring for 4 h. After that, the mixture was dried in a vacuum oven at 60 °C to obtain the final catalyst supported on carbon (named as PdAg-NWs/C and PdNPs/C), available for physical and electrochemical investigations.

2.6. Structural characterization

The samples were dispersed in ethanol by ultrasonication, dropped onto copper grids and dried at room temperature. After that, their morphologies and structure were investigated by transmission electron microscopy (TEM, JEOL 2010, 100 kV) and X-ray diffraction (XRD, D8 X-ray diffractometer, Cu K α radiation). The surface chemistry of the sample was studied using using a Thermo Scientific K-Alpha photoelectron spectrometer (XPS, Al K α X-ray source, 1486.6 eV). The curve-fitting was performed with both symmetric (a mixture of Gaussian/Lorentzian) and asymmetric (modified Lorentzian) line shapes by using Casa XPS software. All spectra were subtracted using a Shirley background. The C 1s binding energy (BE) of 284.5 eV was widely assigned for C-C bond in XC72 [46], thus, this value was applied for the charge correction. Despite of Pd and Ag chemical bonding state, the area ratio of their spin-orbit doublets were fixed at 1.5 while no constraints were applied for the other parameters [47].

2.7. Electrochemical investigation

The electrochemical behaviour of the materials were measured on a Biologic MPG2 potentiostat (France) in a three-electrode cell. A Pt mesh counter electrode and saturated calomel reference electrode (SCE) were used. The working electrode (glassy carbon, GCE, 4 mm diameter) was prepared by polishing with alumina suspensions and ultrasonic cleaning in ethanol. Before each testing, catalyst (3.3 mg) mixed with ethanol (1 mL) for 1h under

ultrasonication, followed by dropping 5 μL of this ink onto GCE and drying at room temperature. A Nafion solution (5 μL , 0.5 wt.% in ethanol) was injected onto the catalyst layer and then air-dried. Cyclic voltammetry (CV) and linear sweep voltammetry (LSV) tests were conducted in 1 M KOH + 1 M $\text{C}_2\text{H}_5\text{OH}$ solution over the potential range from -0.8 to 0.2 V vs SCE (at room temperature, 50 $\text{mV}\cdot\text{s}^{-1}$ scan rate). The current collected from CV and LSV results can be normalized with the utilizing Pd amount to display the mass activity ($\text{mA}\cdot\text{mg}^{-1}_{\text{Pd}}$). The calculation to determine the Pd content in a catalyst sample was detailed in the Supporting Information (Table S1). The poisoning tolerance of catalyst to intermediates was investigated by CO stripping test in 1 M KOH aqueous solution. Firstly, CO gas was bubbled into the solution while keeping the potential at -0.8 V vs SCE for ~ 30 min to saturate CO molecules on the catalysts. Next, in order to remove dissolved CO in solution, switching the gas flux from CO to nitrogen was kept for 10 min. The CO-stripping experiment was proceeded by 10 cycles of CV test from -0.8 V to 0.2 V vs SCE (50 $\text{mV}\cdot\text{s}^{-1}$, room temperature).

3. Results and discussion

3.1. Effect of synthesis temperature

Galvanic replacement reactions have been extensively studied for the synthesis of bimetallic nanocrystals [48]. Here smooth AgNWs (~ 73 nm diameter and ~ 12 μm length, Fig. S2) were employed as the sacrificial templates for the reaction with Pd^{2+} ions. This process includes the diffusion of Pd^{2+} ions to AgNWs' surfaces and then the reduction of Pd^{2+} into Pd(0) depositing on the Ag substrate. Ag atoms of AgNWs are oxidized to Ag^+ ions at the same time. In comparison with previous studies [34, 49], to eliminate the formation of AgCl, which may form attached islands on bimetallic structures, $\text{Pd}(\text{NO}_3)_2\cdot 2\text{H}_2\text{O}$ was used as a precursor to elemental palladium instead of K_2PdCl_4 and PdCl_2 . Moreover, the thermodynamics and the kinetics of a galvanic replacement reaction strongly depend on experimental conditions, e.g., temperature, pH, and concentrations precursors and capping agents. In this work, synthesis temperature was considered as a remarkable influence on the morphology and structure as well as

electrocatalytic activity of PdAg-NWs. As shown in Fig. 1a-e, the distinct architectures, in which Pd played as the outer shell while Ag was the inner core, were generated under the different temperatures. The TEM images also revealed the brighter area than the rest, could be considered as hollow parts of AgNWs. Typically, AgNWs were decorated with several Pd particles at a moderate low temperature (60 °C, Fig. 1a and S3) while the formation of a thin Pd layer with nanoparticles was observed at the higher temperatures (70 °C and 80 °C, Fig. 1b-c). It was noticeable that the Pd layer changed greatly into a rougher morphology with increasing temperature up to 90 °C and 100 °C (Fig. 1d-e). The formation rate of Pd nuclei was available for the deposition rate of Pd particles on AgNWs' surface at temperature below 80 °C. Consequently, a smooth coating with small particles was formed. In contrast, at higher temperatures (90 - 100°C), the reaction took a rapid rate, producing many Pd particles with small sizes as well as large surface energy which tend to dissolve and agglomerate into larger particles on AgNWs' surface due to Ostwald ripening process [50, 51]. It indicates that the synthetic temperature is a crucial parameter to control the architecture of PdAg-NWs.

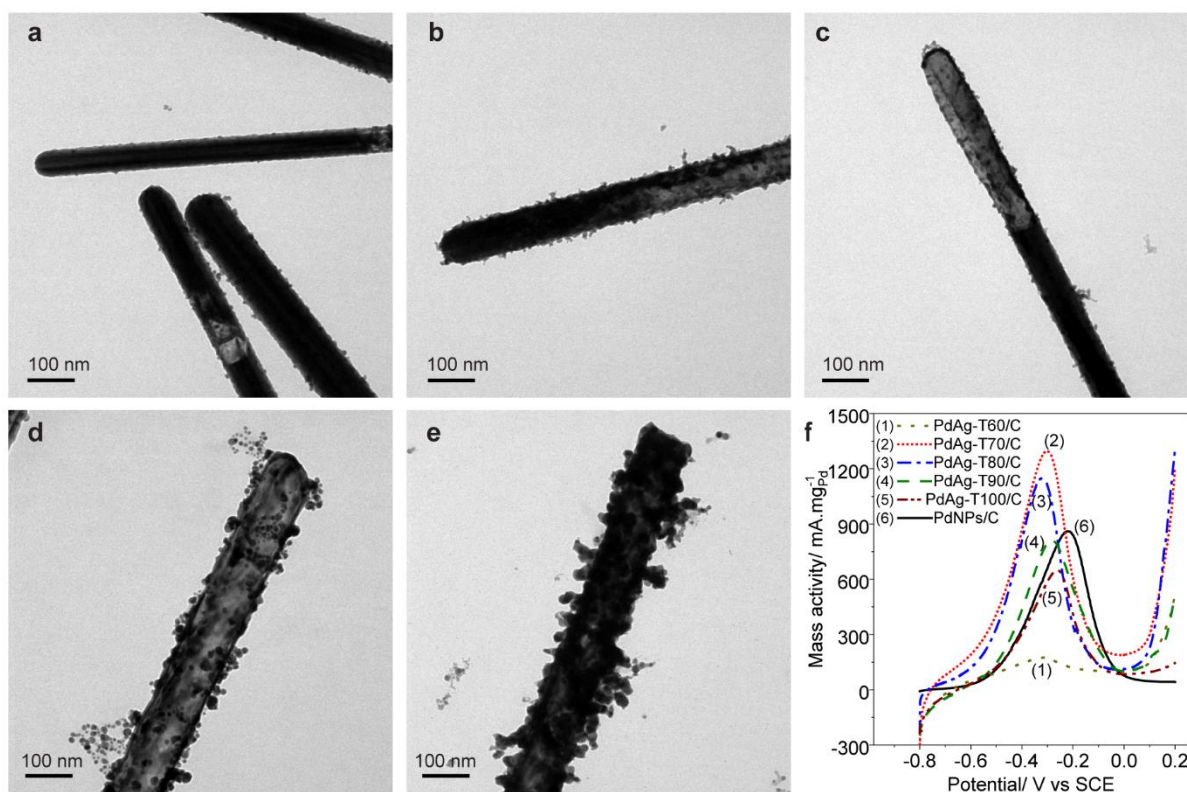


Fig. 1. TEM images of the PdAg-NWs synthesized at different temperatures: (a) 60 °C, (b) 70 °C, (c) 80 °C, (d) 90 °C, and (e) 100 °C for 120 min. (f) LSV curves of the catalysts in (1 M C₂H₅OH + 1 M KOH) solution.

The PdAg-NWs prepared at different temperatures and mixed with XC72 are preferred to as PdAg-T_x/C samples (*x* is the temperature value). The catalytic abilities for the EOR of the PdAg-T_x/C and PdNPs/C samples were investigated with LSV technique in the solution of 1 M C₂H₅OH + 1 M KOH, as shown in Fig. 1f. The LSV curves showed that the catalysts had strong redox peaks in the range of -0.3 to -0.2 V assigned to the ethanol electro-oxidation [22, 32, 52]. The order of the current intensities was PdAg-T60/C < PdAg-T100/C < PdAg-T90/C < PdNPs/C < PdAg-T80/C < PdAg-T70/C. This has confirmed the role of Pd particle configurations on PdAg-NWs' surface in its catalytic properties. A few of decorated structures (PdAg-T60 sample, Fig. 1a) or an agglomeration of clusters (PdAg-T90 and PdAg-T100 samples, Fig. 1d-e) reduced the active sites as well as decreased the interaction between the catalyst and carbon supporter, resulting in inhibiting the catalytic activity. The investigation of the crystalline structures in PtAg nanowires (a similar crystallinity with PdAg-NWs) in previous works proved that the {100} facets occupy most of area along the smooth surface, while others have both {100} and {111} facets [53]. According to Density Functional Theory (DFT) when comparing the electron density at the Pd-Pd bond along the facets, Pd{100} has a higher electron density than the two other facets, hence, the electron transfer from Pd to other agents (e.g., ethanol molecules) is more convenient [54]. Moreover, a previous calculation based on the bonding energy and the bonding length between Pd and O in EOR pointed out that the interactions of Pd{100} with ethanol molecules are stronger than of Pd{111} and Pd{110} [55]. Therefore, well-dispersed and smooth Pd layers in PdAg core-shell nanowires (i.e., PdAg-T70 and PdAg-T80 samples), which have more Pd{100} facets, can improve the adsorption of OH⁻ and ethanol molecules and the EOR rate.

3.2. Effect of synthesis duration

TEM images of the samples prepared for 60 to 180 min, separately, are presented in Fig. S5. It is seen that the PdAg-NWs' surface increases the coverage degree of Pd layer along with an increase in reaction time up to 150 min. After 180 min, some degree of agglomeration of Pd clusters can be observed. In order to examine the electrochemical properties towards ethanol electrooxidation of PdAg-NWs samples, which were synthesized under different times and mixed with XC72 (named as PdAg-ymin/C; y is the synthesis duration), their catalytic activities were measured and further compared with a PdNPs/C catalyst. As shown in Fig. 2, all CVs of PdAg-ymin/C showed peaks at ca. 0.15 V and 0.09 V, corresponding to the Ag(0) oxidation and the Ag(I) reduction, respectively [56]. The intensity of these peaks decreased significantly, i.e., evidences of a decrease in amounts of Ag and an enhanced thickness of Pd coating in PdAg-ymin/C samples, with an increasing reaction time. Remarkably, the I_f/I_b intensity ratio of forward current (I_f) and backward current (I_b) exhibited that all of PdAg-ymin/C samples have $I_f/I_b > 1$ while PdNPs/C has $I_f/I_b < 1$. The low I_f/I_b ratio is generally assumed to be the poor resistance towards poisoned compounds [23, 40], where I_b at ca. -0.41 V is widely assigned to the further oxidation of intermediate carbonaceous compounds, e.g., CH_3CHO , CH_3COOH and CH_3CO^- , formed during the incomplete ethanol oxidation process [1, 57]. However, recent *in situ* surface-enhanced FTIR studies [58] and electrochemical impedance spectroscopy [59] on the methanol oxidation reaction suggested that I_b and I_f/I_b are related to the coverage of free catalytic surface for the oxidation of freshly adsorbed molecules and the degree of oxophilicity, respectively. The exact reason is unclear, but concerns related to the second metal Ag. It is widely agreed that Ag can provide oxygen-containing species to accelerate the oxidation of CO-like species and modify the surface adsorption to enhance the active Pd sites, which are crucial factors to enhance the electrocatalytic activity and stability [6, 22], [60, 61]. The increased activities of the PdAg-NWs with respect to Pd nanocrystals indicate that the presence of Ag improves the EOR performance. As expected, the current intensity of the forward peak at ca. -0.28 V also increased, reaching a maximum at $1652.66 \text{ mA}\cdot\text{mg}^{-1}_{\text{Pd}}$ for PdAg-150min/C,

and then reduced for PdAg-180min/C due to the formation of larger Pd particles. Additionally, the peak potential was the most negative when the synthesis duration was 150 min, indicating that the ethanol was more easily oxidized. Therefore, among the studied PdAg-ymin/C catalysts, PdAg-150min/C has the highest electrocatalytic activity.

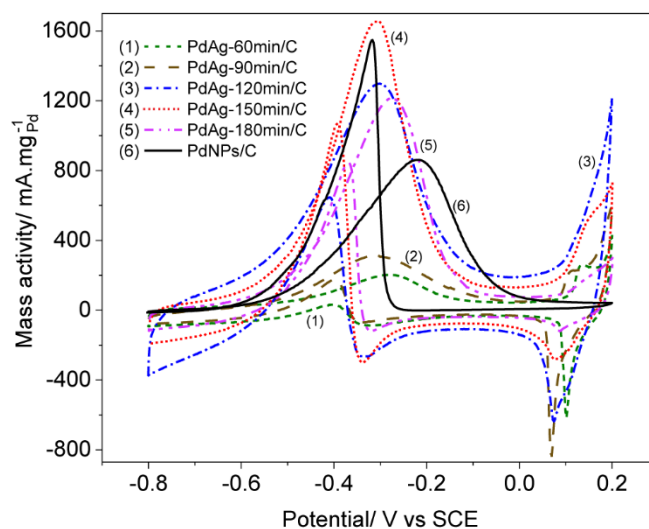
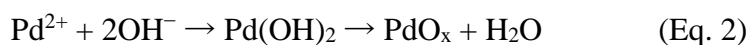
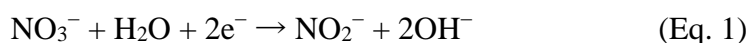


Fig. 2. CV curves of the PdNPs/C and PdAg-ymin/C samples in (1 M C₂H₅OH + 1 M KOH) solution.

3.3. Effect of Pd to Ag molar ratio

The impact of Pd/Ag molar ratios (calculated according to precursors) in the growth of PdNPs on PdAg-NWs (preferred to PdAg-*d*:*g* samples; *d*:*g* is the Pd/Ag molar ratio) is shown clearly in Fig. S6 and S7. Two samples with molar ratios of 10:100 and 12:100 presented a uniform distribution of Pd shells. Meanwhile, at lower ratios of 6:100 and 8:100, only a few PdNPs deposited in a scattered way. The increase of molar ratio up to 14:100 showed unwell-dispersed PdNPs on the AgNWs' surface. Moreover, as shown in Fig. 3a, the XRD patterns of AgNWs and PdAg-NWs exhibited strong diffraction peaks at 38.19°, 44.42° and 64.52°, which could be indexed to (111), (200) and (220), respectively, of a typical face-centered cubic (fcc) lattice of crystalline silver (JCPDS card no. 04-0783). An increasing molar ratio of Pd/Ag from 8:100 to 12:100, although the resulting materials revealed no characteristic peaks of Pd, the peak positions of Ag shifted towards that of Pd.

To eliminate the uncertainty that may be raised, the surface chemistry of PdAg-12:100/C sample was investigated by XPS. As presented in Fig. 3b, there were two well-resolved peaks in the high-resolution spectrum of C1s region in which the most intense one must be assigned to C-C bond of XC72. The remaining peak was found to be positioned at 286.3 eV, corresponding to C-O contamination [46, 62]. There are two peaks located at 368.2 and 374.2 eV in Fig. 3c that should be assigned to the Ag 3d spin-orbit of Ag⁰ [47, 63, 64]. Furthermore, the Pd 3d spectrum (Fig. 3d) showed four distinguished regions, suggesting the presence of at least two different Pd oxidation states. The contribution at 335.2 and 340.5 eV could be easily assigned characteristic peaks of Pd⁰ [62, 65, 66]. These BEs of Pd are higher than that of pure PdNPs, which is an indicator of the formation of PdAg alloy [34]. Moreover, the assignment of the remaining peaks at 337.7, and 343 eV must be assigned for the Pd species that have higher oxidation states (PdO_x). The presence of PdO_x could be explained as follows. During the galvanic replacement process, the electroreduction of NO₃⁻ to NO₂⁻ formed OH⁻ at the substrate (Eq. 1) [67, 68]. Subsequently, the combination of Pd²⁺ and OH⁻ ions easily formed Pd(OH)₂, which deposited on the PdAg-NWs' surface and spontaneously dehydrated into PdO_x (Eq. 2). It was reported that the adsorption of C₂H₅OH and other intermediates could be enhanced in the additional presence of PdO_x layer, resulting in an enhanced productivity [38].



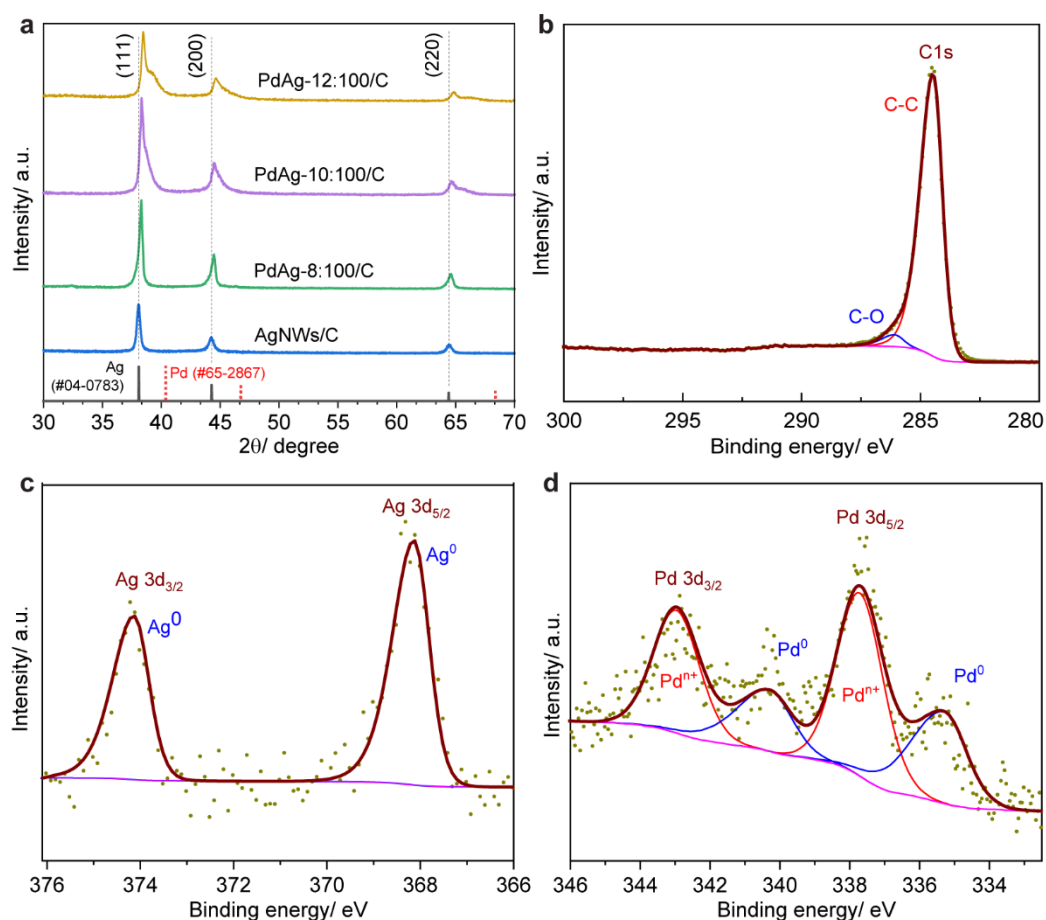


Fig. 3. XRD patterns of the AgNWs and PdAg-*d*:*g* samples (a), and high-resolution XPS spectra of PdAg-12:100/C sample at C1s (b), Ag 3d (c) and Pd 3d (d) core levels.

According to the LSV curves in Fig. 4a, the modification of AgNWs using different Pd contents resulted in an improvement of the electrocatalytic EOR performances. The catalytic capacities of these samples are in the following order: PdAg-6:100/C < PdAg-14:100/C < PdNPs/C < PdAg-8:100/C < PdAg-10:100/C < PdAg-12:100/C. In addition, Fig. 4b showed a comparison of the catalytic activities between them by the current intensities and the onset potential. Encouragingly, the combination of Pd and AgNWs with the Pd/Ag molar ratio of 12:100 (named as PdAg-12:100/C) exhibited the best catalytic ability, shown at the highest intensity (3084.23 mA.mg⁻¹_{Pd}) and the most negative onset potential (-0.64 V). In comparison with PdNPs/C, the intensity and the onset potential of PdAg-12:100/C were 3.58 times greater and 50 mV more negative, respectively.

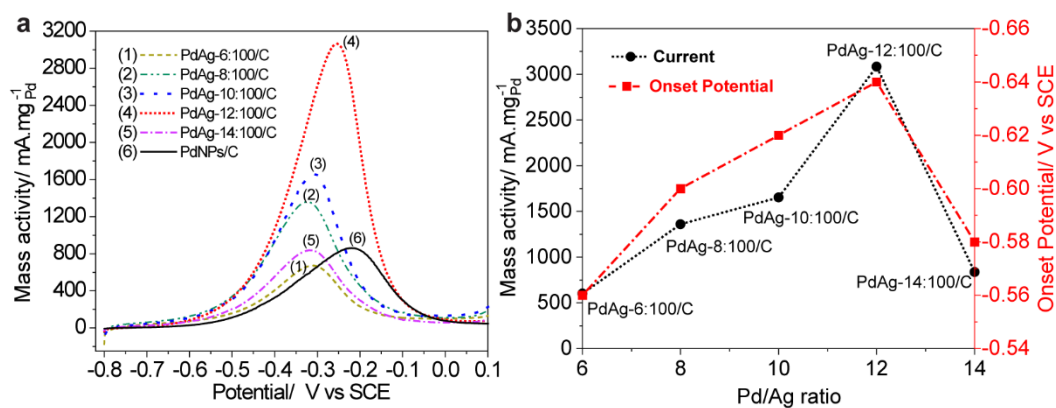


Fig. 4. (a) LSV curves and (b) a comparison of the EOR activities between catalysts synthesized with different Pd/Ag ratios.

3.4. Effect of PVP concentration

It is known that PVP plays important roles not only in protecting and stabilizing the metallic nanoparticles but also in modifying and controlling the limiting non-oriented development of Pd crystals [69, 70]. In this work, the role of PVP in creating a uniform Pd coating for the core-shell structure of PdAg-NWs is shown clearly in Figs. S8 and 5a-b. The samples are referred to PdAg- z PVP, where z is the PVP concentration. The Pd nanoclusters agglomerated into large particles with a using PVP concentration below 0.05% w/v. Meanwhile, a smooth Pd coating on the AgNWs was formed under the PVP solutions from 0.1 to 0.5% w/v. However, excessive PVP molecules hindered the interaction of Pd²⁺ ions with Ag atoms in galvanic replacement reaction, leading to reducing the thickness of Pd layer on AgNWs (Fig. S9). To examine the crystalline lattice structures of Pd and Ag, the high resolution transmission electron microscopy (HRTEM) was applied for PdAg-0.1PVP catalyst as an example (Fig. 5c). The metallic layers were observed with the (200) planes and the corresponding d-spacings identified. It confirms that Pd coating is uniform on AgNWs' surface, and the main facets of PdAg-NWs catalysts are Ag{100}-core and Pd{100}-shell. The uniform distributions of elemental Ag and Pd in PdAg-NWs nanostructures are presented in Fig. 5d-f.

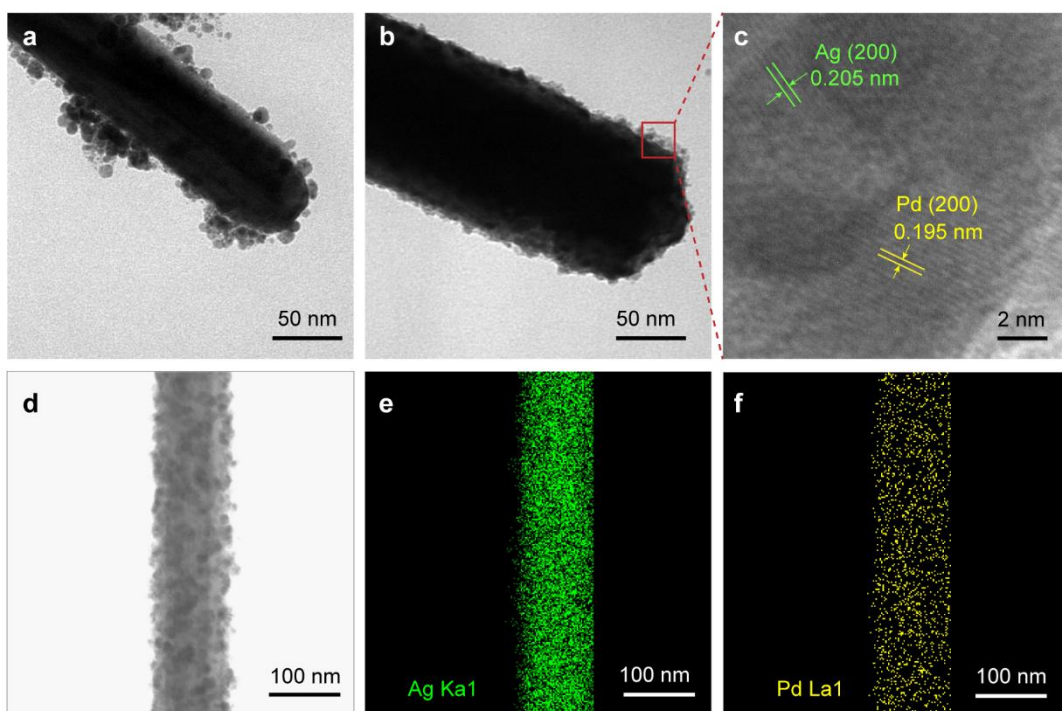


Fig. 5. TEM images of PdAg-NWs synthesized (a) without PVP and (b) in the presence of 0.1% w/v PVP. HRTEM image (c), HAADF-STEM image (d), and EDS elemental mapping for Ag (e) and Pd (f) of PdAg-0.1PVP sample.

From the LSV curves (Fig. 6a), in comparison with PdNPs/C, the samples of PdAg-0PVP/C and PdAg-0.05PVP/C belonged to the group of low catalytic activity due to the aggregation of Pd clusters. Meanwhile, the more active group consisted of PdAg-NWs/C samples synthesized with a PVP concentration of at least 0.1% w/v (smooth layer of Pd on AgNWs, Fig. 5b). As showed in Table S3, when PVP concentration (w/v) increased from 0.1% to 0.5%, I_f decreased from 9744.81 to 1903.84 mA.mg⁻¹_{Pd}, respectively. Typically, the active centers of Pd-based catalysts, which were synthesized in the surfactant solutions (e.g., PVP and polyvinyl alcohol), can be locked by the excess polymers [69, 71]. The amount of Pd in the core-shell structures was also reduced by a high PVP concentration. Therefore, in this study, the EOR activity of PdAg-zPVP/C samples decreased significantly with an increasing PVP concentration (w/v) in the range of 0.1% to 0.5%. The data in Table S3 also showed that all of PdAg-NWs catalysts have $I_f/I_b > 1$, and the onset potentials for EOR reach the most negative at -0.67 V on the PdAg-0.1PVP/C sample. To further investigate the electroactive sites of catalysts, the

electrochemically active surface area (ECSA) was collected by using the coulombic charge of the reduction of PdO in 1 M KOH solution [27, 40]. The results showed that the ECSA value of PdAg-0.1PVP/C, PdAg-0.3PVP/C, PdAg-0.5PVP/C and PdNPs/C were 60.1, 35.8, 30.6 and 22.5 $\text{m}^2 \cdot \text{g}^{-1}_{\text{Pd}}$, respectively. As presented in Fig. 6b, the influence of PVP concentration on the specific activity normalized by ECSA and the mass activity normalized with amount of Pd in catalyst (as calculated in Table S1) is consistent.

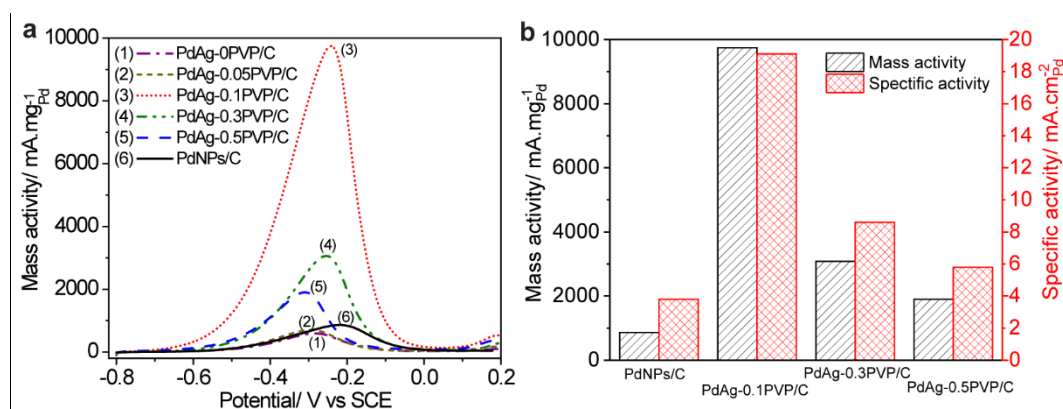


Fig. 6. LSV curves of PdAg-NWs prepared with different PVP concentrations.

The electrochemical impedance spectroscopy (EIS) was also applied to investigate the charge transfer resistances of catalysts. The frequency range was from 10^4 to 1 Hz at a constant potential of -0.3 V and with an amplitude of 10 mV. Nyquist plots of PdAg-zPVP/C and PdNPs/C catalysts in (1 M KOH + 1 M $\text{C}_2\text{H}_5\text{OH}$) solution are presented in Fig. 7. It can be seen that the diameters of the impedance arcs are in the decreasing order of PdNPs/C > PdAg-0.5PVP/C > PdAg-0.3PVP/C > PdAg-0.1PVP/C. According to the Nyquist plots of EIS, a smaller in diameter of the impedance arc of a catalyst is an evidence of a lower charge transfer resistances [40]. As a result, the electro-oxidation of ethanol on the PdAg-0.1PVP/C is more efficient than other samples.

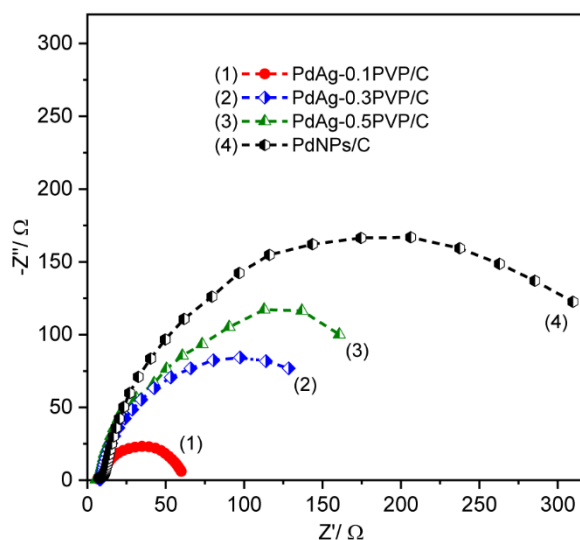


Fig. 7. Nyquist plots of Pd/C and PdAg- z PVP/C catalysts in (1 M KOH + 1 M C₂H₅OH) solution at -0.3 V.

3.5. Investigating the electrochemical durability and the CO poisoning tolerance of catalysts

To examine the durability as well as the poisoning tolerant ability by the intermediate compounds of catalysts, the chronoamperometric (CA) was performed under a constant potential of -0.42 V for 1000 s. From the CA results in Fig. 8, the EOR activities rapidly decreased in the first 100 s, follow by a slow-down at long times. It can be explained that in the early stages, the rapid oxidation of ethanol resulted in a high current intensity, however, the formation of intermediates (e.g., CH₃CO) on the surface also obstructed the catalytic activity. During the reaction time, the metabolic reaction between the intermediates and the final products gradually reached equilibrium, the oxidation reaction slowed down, and the toxicity was limited. We can see the current intensity of the samples in the following order: PdAg-0.05PVP/C < PdAg-0PVP/C < PdNPs/C < PdAg-0.5PVP/C < PdAg-0.3PVP/C < PdAg-0.1PVP/C, this also matches the LSV results in Fig. 6. Thus, after 1000 s, the durable and stable of PdAg-0.1PVP/C sample reached the highest residual intensity (736 mA.mg⁻¹_{Pd}) and 19.4 times higher than PdNPs/C (38 mA.mg⁻¹_{Pd}).

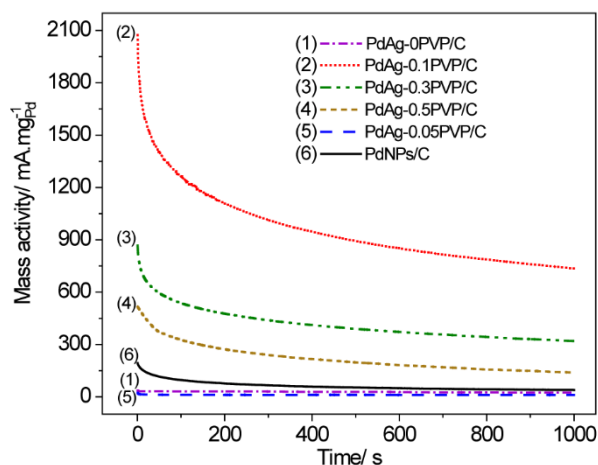


Fig. 8. CA results in (1 M C₂H₅OH + 1 M KOH) solution.

The poisoning tolerance to intermediate species formed during the EOR of PdNPs/C and three PdAg-NWs samples, i.e., PdAg-0.1PVP/C, PdAg-0.3PVP/C and PdAg-0.5PVP/C, was investigated by the CO stripping measurements in a 1 M KOH aqueous solution (Fig. 9). It can be clearly observed that only one strong oxidation peak appeared on the first scan of PdNPs/C meanwhile two oxidation peaks on PdAg-NWs/C are recorded. These data emphasized that two individual active sites which possess different CO-adsorption energy were created on PdAg catalysts [72].

In details, on the forward scan, each sample exhibited a strong peak in the range of -0.17 to -0.10 V which was identified by the electro-oxidation of adsorbed CO molecules on isolated Pd sites [73, 74]. Importantly, one more peak at ca. -0.4 V of each PdAg-zPVP/C catalyst could be the oxidation of CO on PdAg alloy phase formed during the galvanic reaction between Pd(NO₃)₂ and AgNWs [17]. The onset potentials in Table S4 detailed the difference between the samples that is the negative shift of the CO oxidation peak in PdAg-NWs catalysts. The stronger tolerance to CO-like compounds as well as the higher catalytic ability of PdAg-NWs/C than pure PdNPs/C can be explained by the electronic structure modification and bifunctional catalyst according to the Langmuir–Hinshelwood mechanism [75]. Adding other transition metals, e.g., Ru, Ag, Ni, etc. or their oxygen compounds, into Pd-based nanostructures lead to up-shifting of d-band center as well as can provide oxygen-rich species. As a result, the

absorption of OH⁻ groups (OH_{ads}) on their surface is improved, follow by enhancing the oxidation of adsorbed CO molecules (CO_{ads}) on nearby Pd sites [60, 61] as in suggesting Eq. 3 [76]:



The improvement of the OH_{ads} on PdAg-NWs/C can be seen on the forward scan of PdAg-0.1PVP/C (Fig. S10), a broad peak at ca. -0.35 V [57], which disappears on CV result of PdNPs/C. The order of the onset potential for CO electro-oxidation was PdAg-0.1PVP/C < PdAg-0.3PVP/C < PdAg-0.5PVP/C < PdNPs/C. It reveals that PdAg-0.1PVP/C has shown the strongest tolerance to CO-like intermediates.

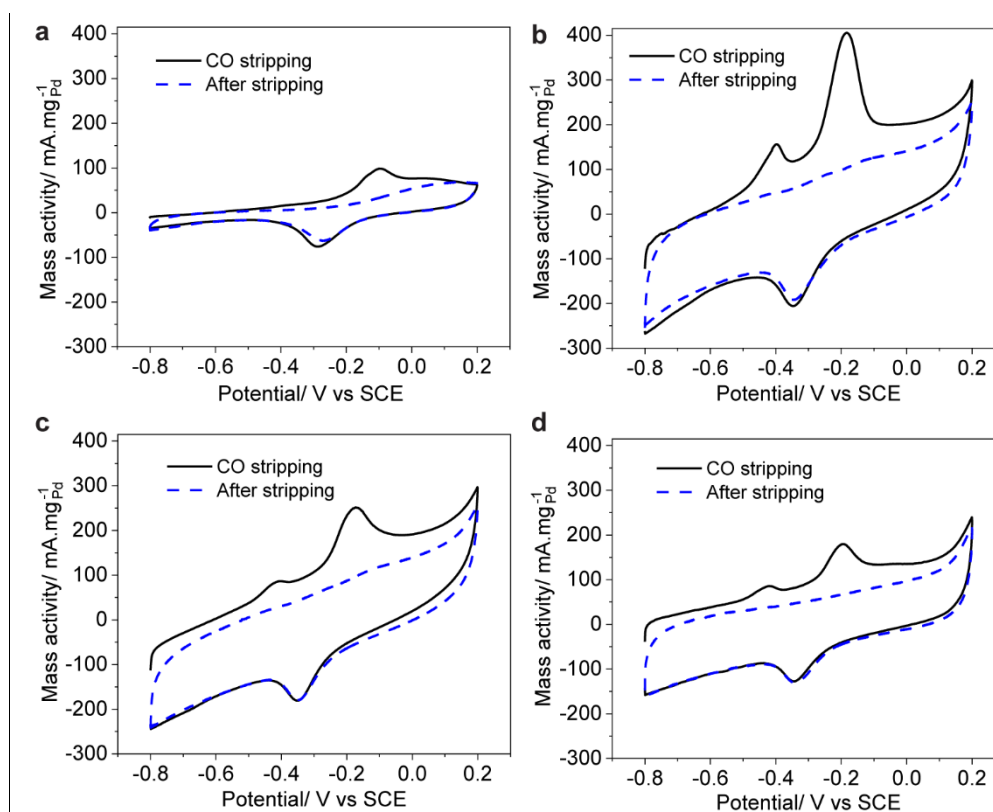


Fig. 9. CO stripping voltammograms of (a) PdNPs/C, (b) PdAg-0.1PVP/C, (c) PdAg-0.3PVP/C, and (d) PdAg-0.5PVP/C in 1 M KOH aqueous solution.

Table 1. Comparative electrochemical properties for EOR of various PdAg-based catalysts

Materials	ECSA $\text{m}^2 \cdot \text{g}^{-1} \text{Pd}$	Current intensity		I_f/I_b ratio	Ref.
		$\text{mA} \cdot \text{mg}^{-1} \text{Pd}$	$\text{mA} \cdot \text{cm}^{-2} \text{Pd}$		
PdAg-0.1PVP/C (nanowires, core Ag - shell Pd, Pd/Ag ratio of 12:100)	60.1	9745	19.1	1.3	This research
PdNPs/C (nanospheres)	22.5	861	3.8	0.6	This research
Pd ₄₀ Ag ₆₀ /C (porous bimetallic dendrites, Pd/Ag ratio of 40:60)	~ 41.8	N.A.	N.A.	N.A.	[41]
PdAg-ANTs/C (alloy nanotubes)	N.A.	N.A.	13.6	1.3	[34]
Commercial Pd/C	N.A.	N.A.	3.38	0.91	[34]
	~24.2	827	N.A.	1.1	[42]
Pd ₂ Ag ₁ -NWs/C (nanowires, Pd/Ag ratio of 2:1)	25.9	2840	11.2	< 1	[16]
PdAgNPs/C (nanodendrites)	69.5	2600	N.A.	>1	[27]
PdAg (nanochains, Pd/Ag ratio of 1:1)	40.2	4098	N.A.	1.3	[42]
PdAg-FPNPs (flower- shaped porous nanoparticles, Pd/Ag ratio of 1:1)	N.A.	N.A.	12.1	< 1	[32]
Pd ₁ Ag ₃ -HNs (hollow nanoflowers, Pd/Ag ratio of 1:3)	25.8	1615.9	N.A.	1.26	[40]

As summarized in [Table 1](#), when compared with the relevant works, the current intensity and the I_f/I_b ratio of the PdAg-0.1PVP/C sample are very competitive. The enhanced electrocatalytic activity of the PdAg-NWs might be correlated to their surface composition, structure and morphology. Firstly, the growth of Pd ($a = 389$ pm) on Ag ($a = 408$ pm) with a different lattice constant can produce tensile strain for the nanostructured PdAg surfaces. This leads to diminish the orbital overlap and alter the width and center of Pd d-band electronic structure [\[77\]](#). Quiang Li group [\[78\]](#) found that the d-band width of Pd in PdAg is more narrowed than in pure Pd, and the Pd d-band center shifts toward the Fermi level due to charge conservation to maintain the degree of d-band filling. As a result, the energy of anti-bonding state for the hybridization between metal d-band and bonding orbital of adsorbates is increased. A lower filling degree of the anti-bonding d state supports a stronger adsorbate-metal binding. Hence, the presence of Ag in PdAg surfaces enriches OH_{ads} on the catalyst sites [\[16, 22, 79-81\]](#), resulting in an enhanced current density, a greater I_f/I_b ratio, and a sooner CO-oxidation ability in CO stripping results of the PdAg-0.1PVP/C sample. Besides, the catalyst with core-shell nanostructures not only minimizes amount of Pd precursor but also improves the electrocatalytic performance. By normalizing the current to the mass of Pd in the catalyst, a low Pd-loading into a uniform Pd-shell along with a partial 1-D hollow AgNW increased significantly its mass activity. The hollow nanostructure can provide more active sites as two sides of the wires, facilitating access and coverage of OH^- species and $\text{C}_2\text{H}_5\text{OH}$ molecules onto the PdAg surfaces [\[15\]](#). Furthermore, the 1D structures of PdAg-NWs, which possess smooth morphologies exposing less surface boundaries and highly selective crystal $\{100\}$ facets [\[16, 82-84\]](#), can facilitate the electron transport. By analyzing the effect of Ag on the surface energy and electronic property of Pd $\{100\}$, Pd $\{110\}$ and Pd $\{111\}$ facets in PdAg [\[78\]](#), it is found that the stability and electric activity of the open-packed $\{100\}$ facet is the most effective. This finding is also confirmed by a higher affinity between Pd $\{100\}$ and O (in $\text{C}_2\text{H}_5\text{OH}$ molecule) rather than the others [\[55\]](#). As shown in our EIS results ([Fig. 7](#)), the highest charge interchange between the PdAg catalysts

and reactants has been achieved in PdAg-0.1PVP/C, i.e., rich in {100} facets. Thus, the reaction kinetics is enhanced and correlates with the significant improvement of the ethanol electro-oxidation on the catalyst surface. The high EOR activity and a strong poisoning tolerance of PdAg-NWs are expected to offer an effective 1D catalyst for applications in the DEFCs.

4. Conclusions

The decorated and core-shell nanostructures of PdAg-NWs with a low Pd/Ag molar ratio were successfully synthesized via a galvanic replacement reaction in polyol media. The synthesis temperature and PVP concentration demonstrated a crucial contribution to control the configuration of Pd layers, while the reaction time and molar ratio of Pd/Ag effectively adjusted the distribution and particle size of PdNPs on 1D AgNWs' surface. Thereby, the decorated or core-shell structures were controllable by tuning these synthesis conditions. As the main advantages of core-shell materials, although utilizing amount of Pd precursor for the preparation of PdAg-NWs was much less than of other PdAg alloys, their electrocatalytic abilities for EOR still performed a high efficiency. The thin Pd coating on Ag-core nanowires, which was fabricated at 70 °C, 150 min, Pd/Ag molar ratio of 12:100 and 0.1% w/v PVP, achieved the highest electrocatalytic activities in EOR. Moreover, by the combination of Pd and 1D AgNWs onto the core-shell structures, their tolerance to CO-like intermediates were better than pure PdNPs. These results make PdAg-NWs a promissory anodic electrocatalyst for direct alcohol alkaline fuel cells.

Acknowledgement

The authors would like to thank Vietnam National Foundation for Science and Technology Development - NAFOSTED for financial support through the project code 104.05-2017.34, the support of time and facilities from Ho Chi Minh City University of Technology (HCMUT), VNU-HCM for this study and Mr. Khoa Dang Vu for his assistance in CV measurement.

References

- [1] Akhairi MAF, Kamarudin SK. Catalysts in direct ethanol fuel cell (DEFC): An overview. *International Journal of Hydrogen Energy*. 2016;41:4214-28.
- [2] Azam AMIN, Lee SH, Masdar MS, Zainoodin AM, Kamarudin SK. Parametric study on direct ethanol fuel cell (DEFC) performance and fuel crossover. *International Journal of Hydrogen Energy*. 2019;44:8566-74.
- [3] Rizo R, Roldan Cuenya B. Shape-Controlled Nanoparticles as Anodic Catalysts in Low-Temperature Fuel Cells. *ACS Energy Letters*. 2019;4:1484-95.
- [4] Mansor M, Timmiati SN, Lim KL, Wong WY, Kamarudin SK, Nazirah Kamarudin NH. Recent progress of anode catalysts and their support materials for methanol electrooxidation reaction. *International Journal of Hydrogen Energy*. 2019;44:14744-69.
- [5] Zhou Y, Wang Z, Liu C. Perspective on CO oxidation over Pd-based catalysts. *Catalysis Science & Technology*. 2015;5:69-81.
- [6] Peng C, Hu Y, Liu M, Zheng Y. Hollow raspberry-like PdAg alloy nanospheres: High electrocatalytic activity for ethanol oxidation in alkaline media. *Journal of Power Sources*. 2015;278:69-75.
- [7] Wang Y, Zou S, Cai W-B. Recent Advances on Electro-Oxidation of Ethanol on Pt- and Pd-Based Catalysts: From Reaction Mechanisms to Catalytic Materials. *Catalysts*. 2015;5:1507-34.
- [8] Badwal SPS, Giddey S, Kulkarni A, Goel J, Basu S. Direct ethanol fuel cells for transport and stationary applications – A comprehensive review. *Applied Energy*. 2015;145:80-103.
- [9] Monyoncho EA, Woo TK, Baranova EA. Ethanol electrooxidation reaction in alkaline media for direct ethanol fuel cells. *Electrochemistry: Volume 15: The Royal Society of Chemistry*; 2019. p. 1-57.

- [10] Rizo R, Sebastián D, Rodríguez JL, Lázaro MJ, Pastor E. Influence of the nature of the carbon support on the activity of Pt/C catalysts for ethanol and carbon monoxide oxidation. *Journal of Catalysis*. 2017;348:22-8.
- [11] Carvalho LL, Colmati F, Tanaka AA. Nickel–palladium electrocatalysts for methanol, ethanol, and glycerol oxidation reactions. *International Journal of Hydrogen Energy*. 2017;42:16118-26.
- [12] Chen W, Zhu Z, Yang L. Palladium nanoparticles supported on a chitosan-functionalized hybrid carbon material for ethanol electro-oxidation. *International Journal of Hydrogen Energy*. 2017;42:24404-11.
- [13] Li C, Yuan Q, Ni B, He T, Zhang S, Long Y, et al. Dendritic defect-rich palladium–copper–cobalt nanoalloys as robust multifunctional non-platinum electrocatalysts for fuel cells. *Nature Communications*. 2018;9:3702.
- [14] Bai J, Liu D, Yang J, Chen Y. Nanocatalysts for Electrocatalytic Oxidation of Ethanol. *ChemSusChem*. 2019;12:2117-32.
- [15] Lv H, Sun L, Lopes A, Xu D, Liu B. Insights into Compositional and Structural Effects of Bimetallic Hollow Mesoporous Nanospheres toward Ethanol Oxidation Electrocatalysis. *The Journal of Physical Chemistry Letters*. 2019;10:5490-8.
- [16] Lv H, Wang Y, Lopes A, Xu D, Liu B. Ultrathin PdAg single-crystalline nanowires enhance ethanol oxidation electrocatalysis. *Applied Catalysis B: Environmental*. 2019;249:116-25.
- [17] Wang Y, Nguyen TS, Liu X, Wang X. Novel palladium–lead (Pd–Pb/C) bimetallic catalysts for electrooxidation of ethanol in alkaline media. *Journal of Power Sources*. 2010;195:2619-22.
- [18] Cai J, Zeng Y, Guo Y. Copper@palladium–copper core–shell nanospheres as a highly effective electrocatalyst for ethanol electro-oxidation in alkaline media. *Journal of Power Sources*. 2014;270:257-61.

- [19] Makin Adam AM, Zhu A, Ning L, Deng M, Zhang Q, Liu Q. Carbon supported PdSn nanocatalysts with enhanced performance for ethanol electrooxidation in alkaline medium. *International Journal of Hydrogen Energy*. 2019;44:20368-78.
- [20] Nguyen ST, Ling Tan DS, Lee J-M, Chan SH, Wang JY, Wang X. Tb promoted Pd/C catalysts for the electrooxidation of ethanol in alkaline media. *International Journal of Hydrogen Energy*. 2011;36:9645-52.
- [21] Tan JL, De Jesus AM, Chua SL, Sanetuntikul J, Shanmugam S, Tongol BJV, et al. Preparation and characterization of palladium-nickel on graphene oxide support as anode catalyst for alkaline direct ethanol fuel cell. *Applied Catalysis A: General*. 2017;531:29-35.
- [22] Nguyen ST, Law HM, Nguyen HT, Kristian N, Wang S, Chan SH, et al. Enhancement effect of Ag for Pd/C towards the ethanol electro-oxidation in alkaline media. *Applied Catalysis B: Environmental*. 2009;91:507-15.
- [23] Oliveira MC, Rego R, Fernandes LS, Tavares PB. Evaluation of the catalytic activity of Pd–Ag alloys on ethanol oxidation and oxygen reduction reactions in alkaline medium. *Journal of Power Sources*. 2011;196:6092-8.
- [24] You H, Gao F, Song T, Zhang Y, Wang H, Liu X, et al. Tunable long-chains of core@shell PdAg@Pd as high-performance catalysts for ethanol oxidation. *Journal of colloid and interface science*. 2020;574:182-9.
- [25] Jiang K, Wang P, Guo S, Zhang X, Shen X, Lu G, et al. Ordered PdCu-Based Nanoparticles as Bifunctional Oxygen-Reduction and Ethanol-Oxidation Electrocatalysts. *Angewandte Chemie International Edition*. 2016;55:9030-5.
- [26] Cui Z, Hu J, Jiang X, Zhang D, Fang C. Asymmetric Au/(PdAg alloy) nano-allium giganteums for their enhanced electrocatalytic performances to ethanol oxidation reaction. *Journal of Alloys and Compounds*. 2021;855:157385.
- [27] Huang W, Kang X, Xu C, Zhou J, Deng J, Li Y, et al. 2D PdAg Alloy Nanodendrites for Enhanced Ethanol Electrooxidation. *Advanced Materials*. 2018;30:1706962.

- [28] Tong Y, Yan X, Liang J, Dou SX. Metal-Based Electrocatalysts for Methanol Electro-Oxidation: Progress, Opportunities, and Challenges. *Small*. 2019;n/a:1904126.
- [29] Liu H, Guo Y, Yu Y, Yang W, Shen M, Liu X, et al. Surface Pd-rich PdAg nanowires as highly efficient catalysts for dehydrogenation of formic acid and subsequent hydrogenation of adiponitrile. *Journal of Materials Chemistry A*. 2018;6:17323-8.
- [30] Hammer B, Nørskov JK. Theoretical surface science and catalysis—calculations and concepts. *Advances in Catalysis*: Academic Press; 2000. p. 71-129.
- [31] Yin Z, Zhang Y, Chen K, Li J, Li W, Tang P, et al. Monodispersed bimetallic PdAg nanoparticles with twinned structures: formation and enhancement for the methanol oxidation. *Scientific reports*. 2014;4:4288.
- [32] Hong W, Wang J, Wang E. Synthesis of porous PdAg nanoparticles with enhanced electrocatalytic activity. *Electrochemistry Communications*. 2014;40:63-6.
- [33] Yang Y, Tian M, Li Q, Min Y, Xu Q, Chen S. Ethanol Electrooxidation Catalyzed by Tungsten Core@Palladium Shell Nanoparticles. *ACS applied materials & interfaces*. 2019;11:30968-76.
- [34] Peng C, Yang W, Wu E, Ma Y, Zheng Y, Nie Y, et al. PdAg alloy nanotubes with porous walls for enhanced electrocatalytic activity towards ethanol electrooxidation in alkaline media. *Journal of Alloys and Compounds*. 2017;698:250-8.
- [35] Huang L, Yang J, Wu M, Shi Z, Lin Z, Kang X, et al. PdAg@Pd core-shell nanotubes: Superior catalytic performance towards electrochemical oxidation of formic acid and methanol. *Journal of Power Sources*. 2018;398:201-8.
- [36] Kakaei K, Dorraji M. One-pot synthesis of Palladium Silver nanoparticles decorated reduced graphene oxide and their application for ethanol oxidation in alkaline media. *Electrochimica Acta*. 2014;143:207-15.
- [37] Ghosh Chaudhuri R, Paria S. Core/Shell Nanoparticles: Classes, Properties, Synthesis Mechanisms, Characterization, and Applications. *Chemical Reviews*. 2012;112:2373-433.

- [38] Krittayavathananon A, Duangdangchote S, Pannopard P, Chanlek N, Sathyamoorthi S, Limtrakul J, et al. Elucidating the unexpected electrocatalytic activity of nanoscale PdO layers on Pd electrocatalysts towards ethanol oxidation in a basic solution. *Sustainable Energy & Fuels*. 2020;4:1118-25.
- [39] Yu X, Luo Z, Zhang T, Tang P, Li J, Wang X, et al. Stability of Pd₃Pb Nanocubes during Electrocatalytic Ethanol Oxidation. *Chemistry of Materials*. 2020;32:2044-52.
- [40] Bin D, Yang B, Zhang K, Wang C, Wang J, Zhong J, et al. Design of PdAg Hollow Nanoflowers through Galvanic Replacement and Their Application for Ethanol Electrooxidation. *Chemistry – A European Journal*. 2016;22:16642-7.
- [41] Jo Y-G, Kim S-M, Kim J-W, Lee S-Y. Composition-tuned porous Pd-Ag bimetallic dendrites for the enhancement of ethanol oxidation reactions. *Journal of Alloys and Compounds*. 2016;688:447-53.
- [42] Feng Y, Zhang K, Yan B, Li S, Du Y. Hydrothermal Method Using DMF as a Reducing Agent for the Fabrication of PdAg Nanochain Catalysts towards Ethanol Electrooxidation. *Catalysts*. 2016;6.
- [43] Nguyen TS, McKeever P, Arredondo-Arechavala M, Wang Y-C, Slater TJA, Haigh SJ, et al. Correlation of the ratio of metallic to oxide species with activity of PdPt catalysts for methane oxidation. *Catalysis Science & Technology*. 2020;10:1408-21.
- [44] Zhu X, Guo Q, Sun Y, Chen S, Wang J-Q, Wu M, et al. Optimising surface d charge of AuPd nanoalloy catalysts for enhanced catalytic activity. *Nature Communications*. 2019;10:1428.
- [45] Cerritos RC, Guerra-Balcázar M, Ramírez RF, Ledesma-García J, Arriaga LG. Morphological Effect of Pd Catalyst on Ethanol Electro-Oxidation Reaction. *Materials*. 2012;5:1686-97.
- [46] Contarini S, Howlett SP, Rizzo C, De Angelis BA. XPS study on the dispersion of carbon additives in silicon carbide powders. *Applied Surface Science*. 1991;51:177-83.

- [47] Moulder JF. Handbook of X-ray Photoelectron Spectroscopy: A Reference Book of Standard Spectra for Identification and Interpretation of XPS Data: Physical Electronics Division, Perkin-Elmer Corporation; 1992.
- [48] Gilroy KD, Ruditskiy A, Peng HC, Qin D, Xia Y. Bimetallic Nanocrystals: Syntheses, Properties, and Applications. *Chem Rev.* 2016;116:10414-72.
- [49] Zhang Y-y, Yi Q-f, Chu H, Nie H-d. Catalytic activity of Pd-Ag nanoparticles supported on carbon nanotubes for the electro-oxidation of ethanol and propanol. *Journal of Fuel Chemistry and Technology.* 2017;45:475-83.
- [50] van Westen T, Groot R. The effect of temperature cycling on Ostwald ripening. *Crystal Growth & Design.* 2018;18.
- [51] Madras G, McCoy B. Temperature effects during Ostwald ripening. *The Journal of Chemical Physics.* 2003;119.
- [52] Nodehi Z, Rafati AA, Ghaffarinejad A. Palladium-silver polyaniline composite as an efficient catalyst for ethanol oxidation. *Applied Catalysis A: General.* 2018;554:24-34.
- [53] Rodrigues TS, da Silva AHM, da Silva AGM, Ceara DG, Gomes JF, Assaf JM, et al. Hollow AgPt/SiO₂ nanomaterials with controlled surface morphologies: is the number of Pt surface atoms imperative to optimize catalytic performances? *Catalysis Science & Technology.* 2016;6:2162-70.
- [54] Kuai L, Geng B, Wang S, Sang Y. A General and High-Yield Galvanic Displacement Approach to Au@M (M=Au, Pd, and Pt) Core-Shell Nanostructures with Porous Shells and Enhanced Electrocatalytic Performances. *Chemistry – A European Journal.* 2012;18:9423-9.
- [55] Wang ED, Xu JB, Zhao TS. Density Functional Theory Studies of the Structure Sensitivity of Ethanol Oxidation on Palladium Surfaces. *The Journal of Physical Chemistry C.* 2010;114:10489-97.

- [56] Feng Y-Y, Liu Z-H, Kong W-Q, Yin Q-Y, Du L-X. Promotion of palladium catalysis by silver for ethanol electro-oxidation in alkaline electrolyte. *International Journal of Hydrogen Energy*. 2014;39:2497-504.
- [57] Liang ZX, Zhao TS, Xu JB, Zhu LD. Mechanism study of the ethanol oxidation reaction on palladium in alkaline media. *Electrochimica Acta*. 2009;54:2203-8.
- [58] Hofstead-Duffy AM, Chen D-J, Sun S-G, Tong YJ. Origin of the current peak of negative scan in the cyclic voltammetry of methanol electro-oxidation on Pt-based electrocatalysts: a revisit to the current ratio criterion. *Journal of Materials Chemistry*. 2012;22:5205-8.
- [59] Chung DY, Lee K-J, Sung Y-E. Methanol Electro-Oxidation on the Pt Surface: Revisiting the Cyclic Voltammetry Interpretation. *The Journal of Physical Chemistry C*. 2016;120:9028-35.
- [60] Brouzgou A, Song SQ, Tsiakaras P. Low and non-platinum electrocatalysts for PEMFCs: Current status, challenges and prospects. *Applied Catalysis B: Environmental*. 2012;127:371-88.
- [61] Chen L, Lu L, Zhu H, Chen Y, Huang Y, Li Y, et al. Improved ethanol electrooxidation performance by shortening Pd–Ni active site distance in Pd–Ni–P nanocatalysts. *Nature Communications*. 2017;8:14136.
- [62] Lupan O, Postica V, Hoppe M, Wolff N, Polonskyi O, Pauporté T, et al. PdO/PdO₂ functionalized ZnO :Pd films for lower operating temperature H₂ gas sensing. *Nanoscale*. 2018;10:14107-27.
- [63] Panafidin MA, Bukhtiyarov AV, Prosvirin IP, Chetyrin IA, Bukhtiyarov VI. Model Bimetallic Pd–Ag/HOPG Catalysts: An XPS and STM Study. *Kinetics and Catalysis*. 2018;59:776-85.
- [64] Pervan P, Milun M. Photoelectron spectroscopy of the Ag/Pd(110) system. *Surface Science*. 1992;264:135-46.

- [65] Militello MC, Simko SJ. Elemental Palladium by XPS. *Surface Science Spectra*. 1994;3:387-94.
- [66] Guerrero-Ortega LPA, Ramírez-Meneses E, Cabrera-Sierra R, Palacios-Romero LM, Philippot K, Santiago-Ramírez CR, et al. Pd and Pd@PdO core-shell nanoparticles supported on Vulcan carbon XC-72R: comparison of electroactivity for methanol electro-oxidation reaction. *Journal of Materials Science*. 2019;54:13694-714.
- [67] Yoshida T, Komatsu D, Shimokawa N, Minoura H. Mechanism of cathodic electrodeposition of zinc oxide thin films from aqueous zinc nitrate baths. *Thin Solid Films*. 2004;451-452:166-9.
- [68] Yang W, Gao Z, Ma J, Wang J, Zhang X, Liu L. Two-step electrodeposition construction of flower-on-sheet hierarchical cobalt hydroxide nano-forest for high-capacitance supercapacitors. *Dalton Transactions*. 2013;42:15706-15.
- [69] Zhao Y, Baeza JA, Koteswara Rao N, Calvo L, Gilarranz MA, Li YD, et al. Unsupported PVA- and PVP-stabilized Pd nanoparticles as catalyst for nitrite hydrogenation in aqueous phase. *Journal of Catalysis*. 2014;318:162-9.
- [70] Yan M, Wu T, Chen L, Yu Y, Liu B, Wang Y, et al. Effect of Protective Agents upon the Catalytic Property of Platinum Nanocrystals. *ChemCatChem*. 2018;10:2433-41.
- [71] Quintanilla A, Butselaar-Orthlieb VCL, Kwakernaak C, Sloof WG, Kreutzer MT, Kapteijn F. Weakly bound capping agents on gold nanoparticles in catalysis: Surface poison? *Journal of Catalysis*. 2010;271:104-14.
- [72] Yang Y, Jin L, Liu B, Kerns P, He J. Direct growth of ultrasmall bimetallic AuPd nanoparticles supported on nitrated carbon towards ethanol electrooxidation. *Electrochimica Acta*. 2018;269:441-51.
- [73] Zhao Y, Zhan L, Tian J, Nie S, Ning Z. Enhanced electrocatalytic oxidation of methanol on Pd/polypyrrole-graphene in alkaline medium. *Electrochimica Acta*. 2011;56:1967-72.

- [74] Zhong J, Bin D, Feng Y, Zhang K, Wang J, Wang C, et al. Synthesis and high electrocatalytic activity of Au-decorated Pd heterogeneous nanocube catalysts for ethanol electro-oxidation in alkaline media. *Catalysis Science & Technology*. 2016;6:5397-404.
- [75] Bao Y, Liu H, Liu Z, Wang F, Feng L. Pd/FeP catalyst engineering via thermal annealing for improved formic acid electrochemical oxidation. *Applied Catalysis B: Environmental*. 2020;274:119106.
- [76] Souza FM, Nandenha J, Batista BL, Oliveira VHA, Pinheiro VS, Parreira LS, et al. Pd_xNb_y electrocatalysts for DEFC in alkaline medium: Stability, selectivity and mechanism for EOR. *International Journal of Hydrogen Energy*. 2018;43:4505-16.
- [77] Gorzkowski MT, Lewera A. Probing the Limits of d-Band Center Theory: Electronic and Electrocatalytic Properties of Pd-Shell–Pt-Core Nanoparticles. *The Journal of Physical Chemistry C*. 2015;119:18389-95.
- [78] Li Q, Song L, Pan L, Chen Y, Ling M, Zhuang X, et al. Density functional theory studies of electronic properties of PdAg/Pd surface alloys. *Applied Surface Science*. 2014;288:69-75.
- [79] Tedsree K, Li T, Jones S, Chan CWA, Yu KMK, Bagot PAJ, et al. Hydrogen production from formic acid decomposition at room temperature using a Ag–Pd core–shell nanocatalyst. *Nature Nanotechnology*. 2011;6:302-7.
- [80] Pettersson LGM, Nilsson A. A Molecular Perspective on the d-Band Model: Synergy Between Experiment and Theory. *Topics in Catalysis*. 2014;57:2-13.
- [81] Greeley J, Nørskov JK. A general scheme for the estimation of oxygen binding energies on binary transition metal surface alloys. *Surface Science*. 2005;592:104-11.
- [82] Cerritos RC, Guerra-Balcázar M, Ramírez RF, Ledesma-García J, Arriaga LG. Morphological Effect of Pd Catalyst on Ethanol Electro-Oxidation Reaction. *Materials*. 2012;5.
- [83] Qi K, Wang Q, Zheng W, Zhang W, Cui X. Porous single-crystalline palladium nanoflowers with enriched {100} facets for highly enhanced ethanol oxidation. *Nanoscale*. 2014;6:15090-7.

[84] Xu CW, Wang H, Shen PK, Jiang SP. Highly Ordered Pd Nanowire Arrays as Effective Electrocatalysts for Ethanol Oxidation in Direct Alcohol Fuel Cells. *Advanced Materials*. 2007;19:4256-9.